

# Proposed Method for use in Launch Condition Optimization

United States Golf Association, R&A Rules Limited

16 March 2021

## 1 Introduction

For a given initial velocity, a golf ball has a corresponding spin and launch angle that will maximize its total distance. The USGA and R&A Rules Ltd. have proposed using these conditions in the evaluation of the conformance of golf balls (USGA/R&A Rules Ltd, 2021 (1)). A method is desired which will efficiently determine optimal launch conditions within prescribed constraints on spin and launch angle. For this work, previously identified constraints for spin and launch angle are used as identified in Table 1.

Table 1: Launch condition constraints

|                    | Min          | Max        |
|--------------------|--------------|------------|
| Spin, RPM (rev/s)  | 2,200 (36.7) | 3,000 (50) |
| Launch Angle, deg. | 7.5          | 15         |

## 2 Method

In order to find the combination of spin and launch which maximizes total distance, a constrained optimization algorithm is used to search the range of conditions. The algorithm used here is the limited-memory Broyden-Fletcher-Goldfarb-Shanno (L-BFGS) optimization method (Nocedal, 1980). The algorithm is in the family of quasi-Newton methods and uses an estimate of the inverse Hessian matrix to search the variable space. The L-BFGS algorithm is implemented using the open-source Accord.Net Framework<sup>1</sup>. This algorithm performed favourably within this domain over other candidate algorithms such as constrained optimization by linear approximation (COBYLA) (Powell, 1994) and the augmented Lagrangian method.

## 3 Optimization

To ensure the algorithm has found the optimum launch conditions within the prescribed boundaries the solution is compared here with the results of a high-resolution grid search. The grid search finds the total distance for a large number of evenly spaced initial conditions within the prescribed spin and launch boundaries. The spacing used is 30 RPM (0.5 rev/s) and 0.25° between each launch condition. Thus, 868 combinations from (2,200 RPM/36.7 rev/s, 7.5°) to

---

<sup>1</sup> <http://accord-framework.net>

(3,000 RPM/50.0 rev/s, 15°) are tested to find the conditions yielding the maximum total distance.

A sample of 121 golf balls for which detailed aerodynamic data are available over a broad range of speed and spin were simulated in poles horizontal and pole-over-pole orientation under environmental conditions set forth by (R&A Rules, Ltd./USGA, 2019), 75 °F, 30 in. Hg, 50% relative humidity and at an assumed initial velocity of 256 ft/s. The bounce model used is provided in Equation 1 (USGA/R&A Rules Ltd, 2021 (2)), with  $\alpha_f$  being the terminal angle and  $d_{bounce}$  equal to the distance of the bounce and roll.

$$d_{bounce} = 79.1 - 1.6|\alpha_f| \quad (1)$$

Within the set of 241 simulated shots the mean difference between the grid search and the algorithm was 0.007 yards, with a maximum difference of 0.13 yards. Figure 1 shows the difference in solutions between a grid search and the L-BFGS algorithm for an individual ball.

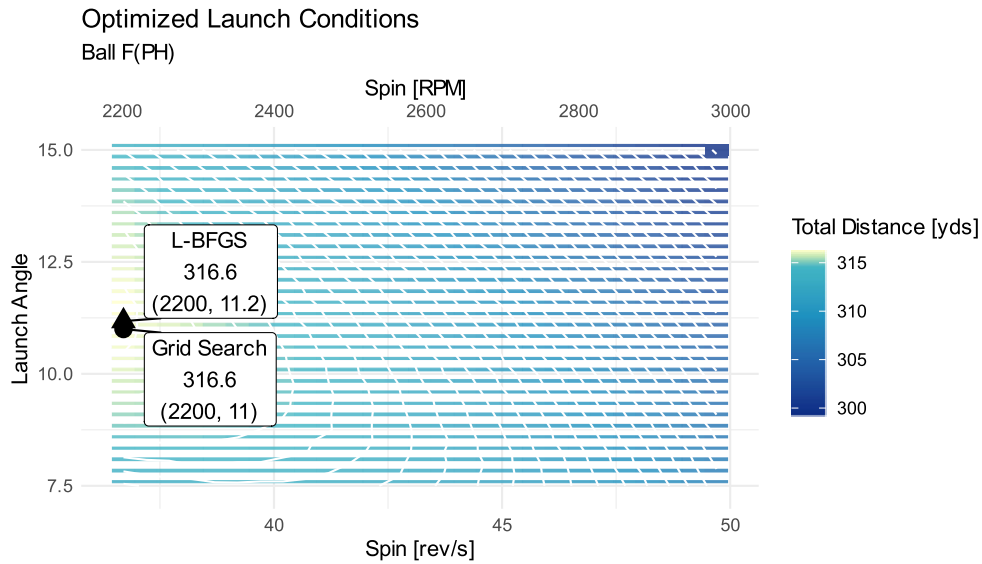


Figure 1: This sample showed a difference between the L-BFGS algorithm and a grid search of 0.03 yards. The difference in launch angle is 0.18 degrees (Ball F(PH)).

In comparison of both methods, most balls simulated found the optimum spin to be on the boundary of 2,200 RPM (36.7 rev/s), as can be seen in the summary of results in Table 2. Approximately 90% of balls showed agreement in launch angle optimum to within 0.50 degrees. Those balls which showed a larger disagreement in optimum conditions showed a large plateau region in which changes to spin and launch could be changed without affecting the resultant total distance. An example of a large total plateau and the resulting algorithm predictions are shown in Figure 2.

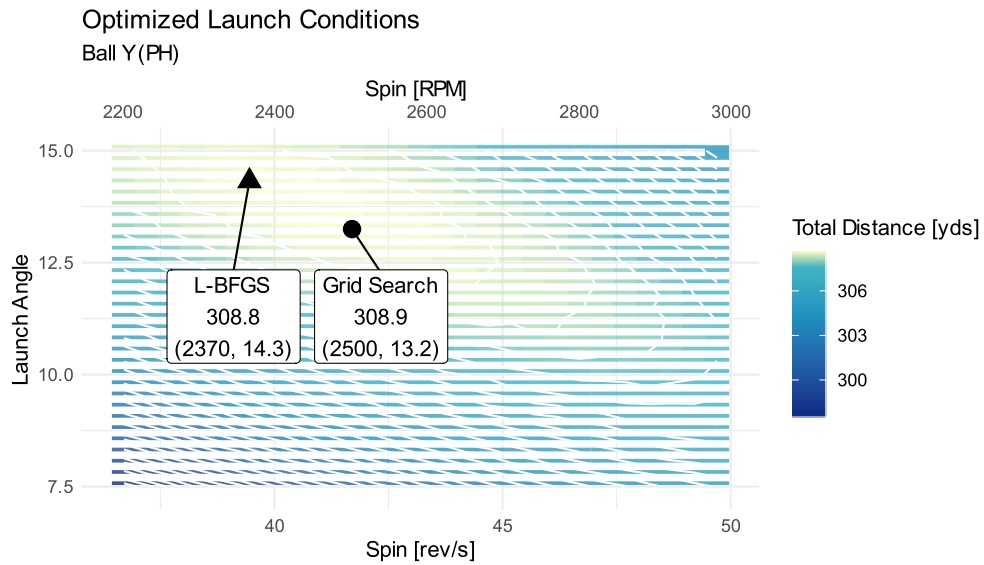


Figure 2: Largest disagreement observed over the simulated golf balls showed a difference of 1.1 degrees and 130 RPM (ball Y(PH)). However, due to the large plateau region of total distance, the resulting distance difference was 0.05 yards.

Table 2: Results 15 samples simulated. Differences = Grid – L-BFGS.  
\*Results are those shown in Figure 1 and Figure 2.

| Ball Id | Grid Search        |           |                 | L-BFGS             |           |                 | Differences        |           |                 |
|---------|--------------------|-----------|-----------------|--------------------|-----------|-----------------|--------------------|-----------|-----------------|
|         | Launch angle, deg. | Spin, RPM | Distance, yards | Launch angle, deg. | Spin, RPM | Distance, yards | Launch angle, deg. | Spin, RPM | Distance, yards |
| A(PH)   | 13.0               | 2,200     | 312.1           | 13.1               | 2,200     | 312.1           | -0.1               | 0         | 0.0             |
| A(PP)   | 10.5               | 2,200     | 309.2           | 10.5               | 2,200     | 309.2           | 0.0                | 0         | 0.0             |
| B(PH)   | 11.8               | 2,200     | 312.1           | 12.0               | 2,200     | 312.1           | -0.2               | 0         | 0.0             |
| B(PP)   | 10.8               | 2,200     | 309.8           | 10.8               | 2,200     | 309.8           | 0.0                | 0         | 0.0             |
| C(PH)   | 11.8               | 2,200     | 313.9           | 12.3               | 2,200     | 313.9           | -0.5               | 0         | 0.0             |
| C(PP)   | 10.0               | 2,200     | 314.4           | 10.2               | 2,200     | 314.4           | -0.2               | 0         | 0.0             |
| D(PH)   | 12.5               | 2,200     | 313.3           | 12.6               | 2,200     | 313.4           | -0.1               | 0         | -0.1            |
| D(PP)   | 11.3               | 2,200     | 314.7           | 11.5               | 2,200     | 314.7           | -0.2               | 0         | 0.0             |
| E(PH)   | 12.0               | 2,200     | 314.4           | 11.9               | 2,200     | 314.4           | 0.1                | 0         | 0.0             |
| E(PP)   | 9.8                | 2,200     | 314.1           | 9.3                | 2,200     | 314.0           | 0.5                | 0         | 0.1             |
| F*(PH)  | 11.0               | 2,200     | 316.6           | 11.2               | 2,200     | 316.6           | -0.2               | 0         | 0.0             |
| F(PP)   | 9.3                | 2,200     | 313.5           | 9.2                | 2,200     | 313.5           | 0.1                | 0         | 0.0             |
| G(PH)   | 13.5               | 2,200     | 311.0           | 12.8               | 2,200     | 311.1           | 0.7                | 0         | -0.1            |
| G(PP)   | 12.0               | 2,200     | 310.9           | 12.1               | 2,200     | 310.9           | -0.1               | 0         | 0.0             |
| Y*(PH)  | 13.2               | 2,500     | 308.9           | 14.3               | 2,370     | 308.8           | -1.1               | 130       | 0.1             |

Finally, compared to the intensive grid search, the use of an optimization method yields significant improvements in efficiency, with a tenfold reduction in processing time (Table 3).

Table 3: Optimization efficiency. \*Intel i7-9850H 2.60 GHz

|             | Function<br>evaluations | Computation<br>Time*, seconds<br>(average) |
|-------------|-------------------------|--|
| Grid search | 868                     | 36   |
| L-BFGS      | 53                      | 3.4  |

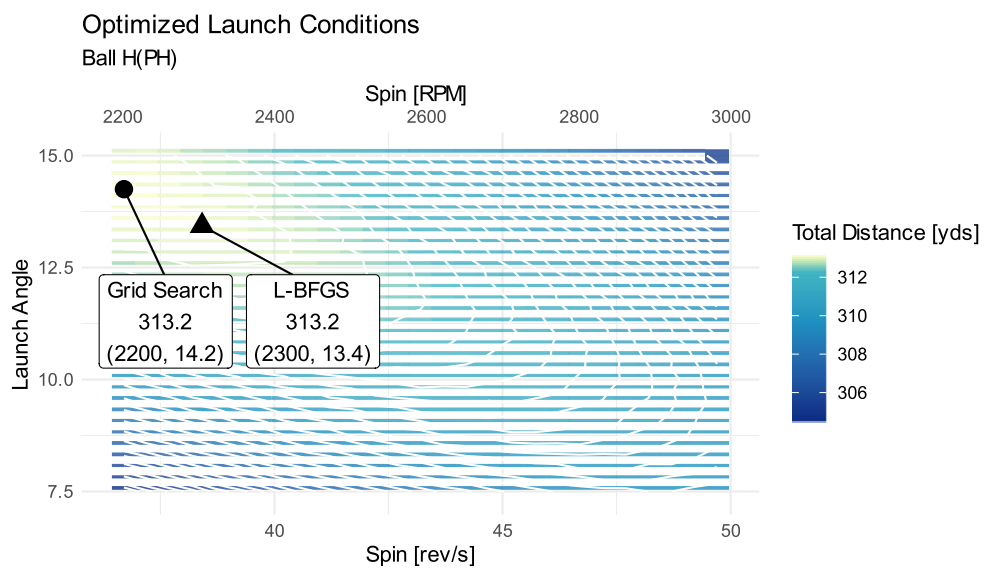
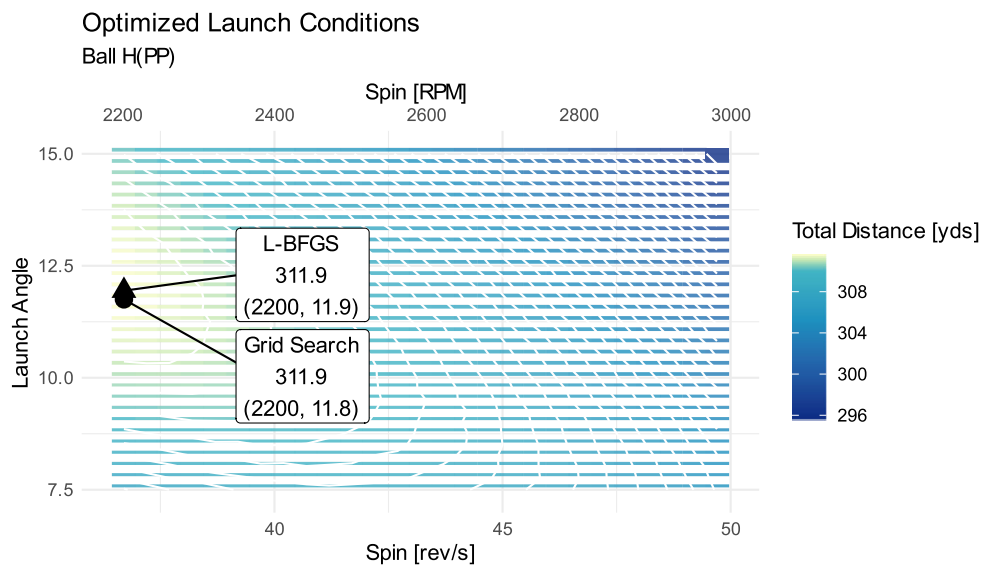
## 4 Conclusion

The described method provides an effective path to obtain optimized launch conditions under spin and launch constraints. The algorithm yields highly accurate results in comparison with a high-resolution grid search, at times even improving upon the grid solution. A maximum difference of 0.13 yards was observed in optimized total distance between these methods for the balls sampled. While predicted optimal spin and launch differed on occasion, these differences were observed to fall within a plateau region where changes to spin and launch do not strongly affect total distance.

## 5 References

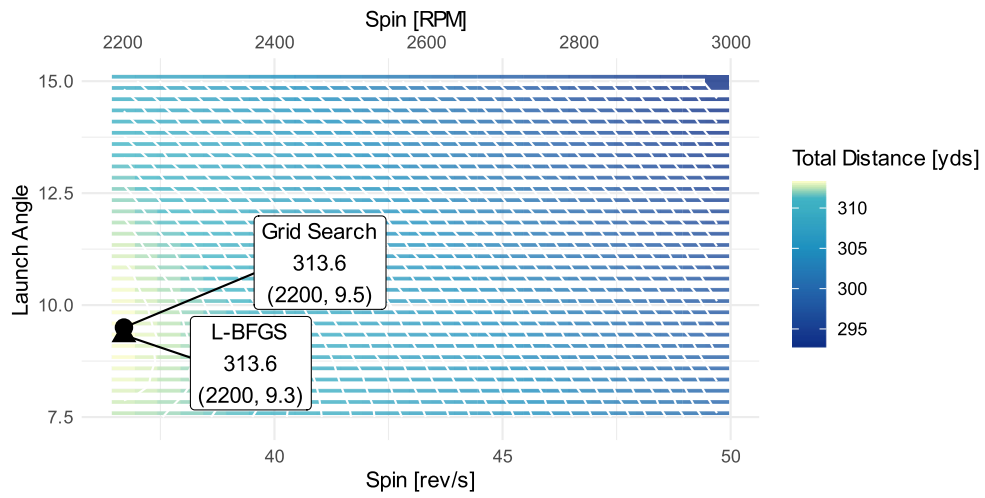
- Nocedal, J. (1980, July). Updating Quasi-Newton Matrices with Limited Storage. *Mathematics of Computation*, 35(151), 773-782. doi:10.2307/2006193
- Powell, M. J. (1994). A Direct Search Optimization Method That Models the Objective and Constraint Functions by Linear Interpolation. *Advances in Optimization and Numerical Analysis*, 51-67. doi:10.1007/978-94-015-8330-5\_4
- R&A Rules, Ltd./USGA. (2019). *Overall Distance and Symmetry Test Procedure*. St Andrews, Liberty Corner: R&A Rules, Ltd., United States Golf Association.
- USGA/R&A Rule Ltd. (2021). *A simplified bounce model for evaluating optimum overall distance*. Liberty Corner, St Andrews: United States Golf Association, R&A Rules Ltd.
- USGA/R&A Rules Ltd. (2021). *Notice to Manufacturers*. Liberty Corner, St Andrews: United States Golf Association, R&A Rules, Ltd.

## 6 Appendix



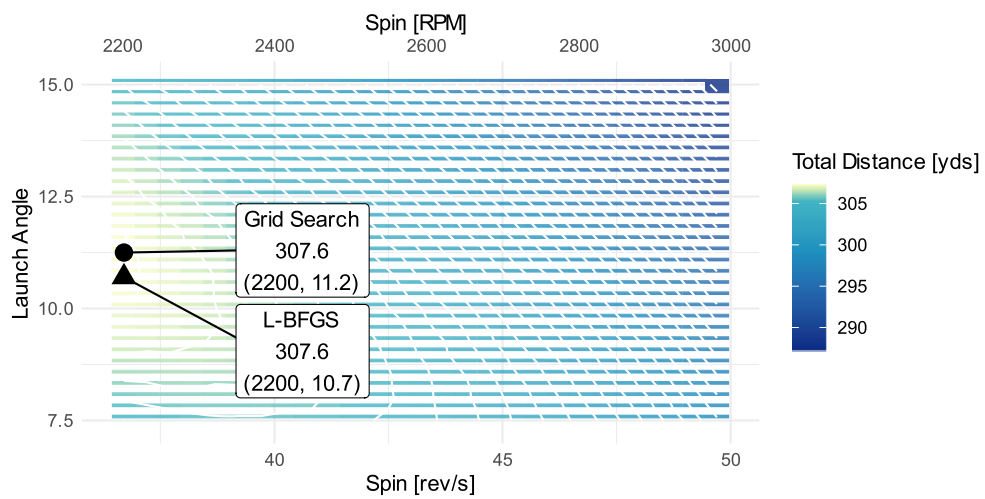
### Optimized Launch Conditions

Ball I (PP)



### Optimized Launch Conditions

Ball M (PH)



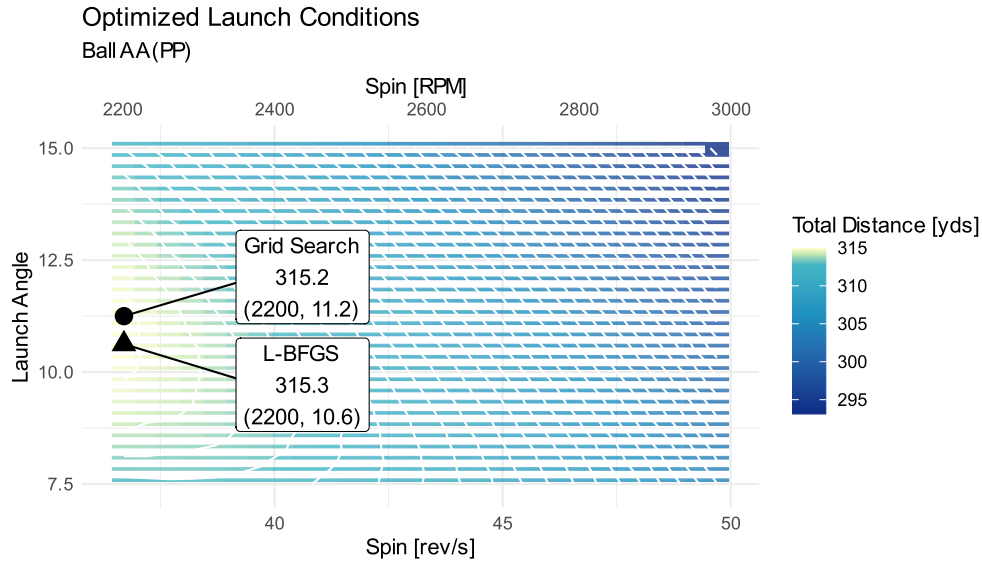


Figure 3: Selected distance contours with indication of dense-grid and L-BFGS optima.

Table 4: Comparison of the first 50 results between a grid search and the L-BFGS algorithm. Note some balls have a negative distance difference. These are locations that L-BFGS improved upon the high-resolution grid search results.  
\*There is a corresponding figure in the document.

| Grid Search |                    |           | L-BFGS          |                    |           | Differences     |                    |           |                 |
|-------------|--------------------|-----------|-----------------|--------------------|-----------|-----------------|--------------------|-----------|-----------------|
| Ball Id     | Launch angle, deg. | Spin, RPM | Distance, yards | Launch angle, deg. | Spin, RPM | Distance, yards | Launch angle, deg. | Spin, RPM | Distance, yards |
| A(PH)       | 13.0               | 2,200     | 312.1           | 13.1               | 2,200     | 312.1           | -0.1               | 0         | 0.0             |
| A(PP)       | 10.5               | 2,200     | 309.2           | 10.5               | 2,200     | 309.2           | 0.0                | 0         | 0.0             |
| B(PH)       | 11.8               | 2,200     | 312.1           | 12.0               | 2,200     | 312.1           | -0.2               | 0         | 0.0             |
| B(PP)       | 10.8               | 2,200     | 309.8           | 10.8               | 2,200     | 309.8           | 0.0                | 0         | 0.0             |
| C(PH)       | 11.8               | 2,200     | 313.9           | 12.3               | 2,200     | 313.9           | -0.5               | 0         | 0.0             |
| C(PP)       | 10.0               | 2,200     | 314.4           | 10.2               | 2,200     | 314.4           | -0.2               | 0         | 0.0             |
| D(PH)       | 12.5               | 2,200     | 313.3           | 12.6               | 2,200     | 313.4           | -0.1               | 0         | -0.1            |
| D(PP)       | 11.3               | 2,200     | 314.7           | 11.5               | 2,200     | 314.7           | -0.2               | 0         | 0.0             |
| E(PH)       | 12.0               | 2,200     | 314.4           | 11.9               | 2,200     | 314.4           | 0.1                | 0         | 0.0             |
| E(PP)       | 9.8                | 2,200     | 314.1           | 9.3                | 2,200     | 314.0           | 0.5                | 0         | 0.1             |
| F(PH)       | 11.0               | 2,200     | 316.6           | 11.2               | 2,200     | 316.6           | -0.2               | 0         | 0.0             |
| F(PP)       | 9.3                | 2,200     | 313.5           | 9.2                | 2,200     | 313.5           | 0.1                | 0         | 0.0             |
| G(PH)       | 13.5               | 2,200     | 311.0           | 12.8               | 2,200     | 311.1           | 0.7                | 0         | -0.1            |
| G(PP)       | 12.0               | 2,200     | 310.9           | 12.1               | 2,200     | 310.9           | -0.1               | 0         | 0.0             |
| H*(PH)      | 14.2               | 2,200     | 313.2           | 13.4               | 2,300     | 313.2           | 0.8                | -100      | 0.0             |
| H*(PP)      | 11.8               | 2,200     | 311.9           | 11.9               | 2,200     | 311.9           | -0.1               | 0         | 0.0             |
| I(PH)       | 11.0               | 2,200     | 312.9           | 10.6               | 2,200     | 313.0           | 0.4                | 0         | -0.1            |
| I*(PP)      | 9.5                | 2,200     | 313.6           | 9.3                | 2,200     | 313.6           | 0.2                | 0         | 0.0             |
| J(PH)       | 10.5               | 2,200     | 315.3           | 10.4               | 2,200     | 315.3           | 0.1                | 0         | 0.0             |
| J(PP)       | 9.5                | 2,200     | 313.6           | 9.2                | 2,200     | 313.7           | 0.3                | 0         | -0.1            |

| Ball Id | Launch angle, deg. | Spin, RPM | Distance, yards | Launch angle, deg. | Spin, RPM | Distance, yards | Launch angle, deg. | Spin, RPM | Distance, yards |
|---------|--------------------|-----------|-----------------|--------------------|-----------|-----------------|--------------------|-----------|-----------------|
| K(PH)   | 10.8               | 2,200     | 317.5           | 10.8               | 2,200     | 317.5           | 0.0                | 0         | 0.0             |
| K(PP)   | 10.0               | 2,200     | 314.6           | 10.1               | 2,200     | 314.7           | -0.1               | 0         | -0.1            |
| L(PH)   | 10.5               | 2,200     | 316.5           | 10.4               | 2,200     | 316.5           | 0.1                | 0         | 0.0             |
| M*(PH)  | 11.2               | 2,200     | 307.6           | 10.7               | 2,200     | 307.6           | 0.5                | 0         | 0.0             |
| M(PP)   | 11.0               | 2,200     | 310.5           | 10.6               | 2,200     | 310.5           | 0.4                | 0         | 0.0             |
| N(PH)   | 13.5               | 2,200     | 306.7           | 13.1               | 2,300     | 306.7           | 0.4                | -100      | 0.0             |
| N(PP)   | 12.8               | 2,200     | 304.8           | 12.6               | 2,200     | 304.8           | 0.2                | 0         | 0.0             |
| O(PH)   | 9.0                | 2,200     | 310.7           | 8.9                | 2,200     | 310.7           | 0.1                | 0         | 0.0             |
| O(PP)   | 11.0               | 2,200     | 313.7           | 10.7               | 2,200     | 313.7           | 0.3                | 0         | 0.0             |
| P(PH)   | 9.5                | 2,200     | 310.5           | 9.6                | 2,200     | 310.6           | -0.1               | 0         | -0.1            |
| P(PP)   | 10.8               | 2,200     | 313.0           | 10.7               | 2,200     | 313.0           | 0.1                | 0         | 0.0             |
| Q(PH)   | 8.5                | 2,200     | 310.5           | 8.7                | 2,200     | 310.5           | -0.2               | 0         | 0.0             |
| Q(PP)   | 11.0               | 2,200     | 313.3           | 10.7               | 2,200     | 313.4           | 0.3                | 0         | -0.1            |
| R(PH)   | 13.0               | 2,200     | 313.7           | 13.1               | 2,200     | 313.7           | -0.1               | 0         | 0.0             |
| R(PP)   | 11.0               | 2,200     | 311.7           | 10.7               | 2,200     | 311.8           | 0.3                | 0         | -0.1            |
| S(PH)   | 12.0               | 2,200     | 312.3           | 11.7               | 2,200     | 312.3           | 0.3                | 0         | 0.0             |
| S(PP)   | 9.8                | 2,200     | 312.1           | 10.0               | 2,200     | 312.2           | -0.2               | 0         | -0.1            |
| T(PH)   | 11.5               | 2,200     | 306.5           | 11.4               | 2,200     | 306.5           | 0.1                | 0         | 0.0             |
| T(PP)   | 12.0               | 2,200     | 311.4           | 11.8               | 2,200     | 311.4           | 0.2                | 0         | 0.0             |
| U(PH)   | 10.0               | 2,200     | 315.5           | 9.6                | 2,200     | 315.4           | 0.4                | 0         | 0.1             |
| U(PP)   | 7.8                | 2,200     | 313.2           | 7.6                | 2,200     | 313.2           | 0.2                | 0         | 0.0             |
| V(PH)   | 11.0               | 2,200     | 317.6           | 10.6               | 2,200     | 317.6           | 0.4                | 0         | 0.0             |
| V(PP)   | 8.0                | 2,200     | 314.2           | 7.9                | 2,200     | 314.2           | 0.1                | 0         | 0.0             |
| W(PH)   | 13.8               | 2,230     | 309.7           | 13.2               | 2,270     | 309.7           | 0.6                | -40       | 0.0             |
| W(PP)   | 11.3               | 2,200     | 306.9           | 11.4               | 2,200     | 306.9           | -0.1               | 0         | 0.0             |
| X(PH)   | 12.3               | 2,200     | 309.8           | 12.1               | 2,210     | 309.8           | 0.2                | -10       | 0.0             |
| X(PP)   | 12.0               | 2,200     | 310.3           | 11.6               | 2,210     | 310.3           | 0.4                | -10       | 0.0             |
| Y*(PH)  | 13.2               | 2,500     | 308.9           | 14.3               | 2,370     | 308.8           | -1.1               | 130       | 0.1             |
| Y(PP)   | 12.5               | 2,200     | 306.8           | 12.5               | 2,260     | 306.7           | 0.0                | -60       | 0.1             |
| Z(PH)   | 12.5               | 2,200     | 311.7           | 12.8               | 2,200     | 311.7           | -0.3               | 0         | 0.0             |
| AA*(PP) | 11.2               | 2,200     | 315.2           | 10.6               | 2,200     | 315.3           | 0.6                | 0         | -0.1            |